Characterization of La-Doped TiO₂ Nanopowders by Raman Spectroscopy

M. Šćepanović[a,*], S. Aškrabić[a], V. Berec[a], A. Golubović[a], Z. Dohčević-Mitrović[a],

A. Kremenović[b] and Z.V. Popović[a]

[a]Center for Solid State Physics and New Materials, Institute of Physics

Pregrevica 118, 11080 Belgrade, Serbia

[b]Faculty of Mining and Geology, Laboratory for Crystallography

University of Belgrade, Djušina 7, 11000 Belgrade, Serbia

Titanium dioxide (TiO_2) nanopowders doped with 0.65, 1, 2, 3 and 4 wt.% of lanthanum ions (La^{3+}) were synthesized by sol-gel technology. Dependence of structural and morphological characteristics of nanopowders on La^{3+} content and synthesis conditions is investigated by the Raman spectroscopy. Very intensive modes observed in the Raman spectra of all nanopowder samples are assigned to anatase phase of TiO_2. Additional Raman modes of extremely low intensity can be related to the presence of certain amount of highly disordered brookite phase in nanopowders. Dependence of the intensity ratio of the Raman modes which originate from anatase and brookite on doping conditions is specially analyzed. In order to estimate the variation of nanocrystallite size with dopant content, shift and asymmetrical broadening of the most intensive E_g Raman mode of anatase are analyzed by phonon confinement model. The obtained results are compared with the results of X-ray diffraction spectroscopy. Special attention is dedicated to the changes in the Raman spectra of pure and La-doped TiO_2 nanopowders observed after high temperature treatment.

PACS numbers: 81.20.Fw, 81.07.Wx, 78.30.−j, 07.05.Tp

1. Introduction

Titanium dioxide has three polymorphs: rutile (tetragonal, $P42/mnm$), anatase (tetragonal, $I41/amd$), and brookite (orthorhombic, $Pbca$). All of them have numerous applications as important industrial materials. In recent years, nanosized TiO_2, especially anatase TiO_2, has attracted much attention as key material for photocatalysts [1], dye-sensitized solar cells [2], gas sensors [3] and electrochromic devices [4]. The applications of nanosized anatase TiO_2 are primarily determined by its physicochemical properties such as crystalline structure, particle size, surface area, porosity and thermal stability. The aim of this paper is to investigate the variations in structure of anatase nanopowders, synthesized by sol-gel method, induced by doping with lanthanum. Structural properties, such as: existence of mixed phases (anatase in combination with considerable amount of rutile or brookite phase), particle size and particle size distribution, as well as value and type of the strain (compressed or tensile) determined by the Raman spectroscopy are correlated to the content of La-dopant.

2. Experimental details

$TiCl_4$ was used as the precursor in the synthesis process. The $Ti(OH)_4$ hydrogel was obtained by hydrolysis of $TiCl_4$ at 0°C with controlled addition of 2.5 wt.% aqueous ammonia into the aqueous solution of $TiCl_4$ (0.3 mol/l) and careful control of the pH value of the solution (9.3). $TiCl_4$ is soluble in water but it experiences rigorous reaction at 20°C which can be very important to perform this reaction at lower temperature. After aging in the mother liquor for 5 h, the as-prepared hydrogel was filtered and washed out with deionized water until complete removal of chlorine ions. The obtained $Ti(OH)_4$ hydrogel was converted to its ethanol-gel by repeated exchange with anhydrous ethanol for several times (by repeated introduction of anhydrous ethanol). The obtained alcogel represents the starting point for production of TiO_2 nanoparticles. Alcogel was placed in a vessel, dried at 280°C and calcined at temperature of 550°C, after which it was converted to the nanoparticles. In the case of La-doped TiO_2, $LaCl_3 \cdot 7H_2O$ was used. All chemicals used in this experiment were analytical grades (Merck Chemicals) and were used as received.

Powder X-ray diffraction (XRD) was used for the identification of crystalline phases, quantitative phase analysis and estimation of crystallite size and strain. The XRD patterns were collected on a Philips diffractometer (PW1710) employing Cu $K_{\alpha_{1,2}}$ radiation. Step scanning was performed with 2θ ranging from 10 to 135°, step size of 0.06° and the fixed counting time of 41 s/step. The XRD patterns were used to refine crystallographic structure and microstructural parameters using the procedure explained elsewhere [5, 6]. The Fullprof computer program was used [5].

---

* corresponding author; e-mail: maja@phy.bg.ac.yu

The Raman measurements were performed at room temperature using the Jobin-Yvon T64000 triple spectrometer system, equipped with confocal microscope and a nitrogen-cooled CCD detector. The 514 nm laser line of an Ar^+ laser was used as an excitation source.

3. Results and discussion

Relevant and the most intensive diffraction peaks in the XRD patterns of all samples belong to anatase crystal structure of TiO_2 (JCPDS card 78-2486). The patterns of pure TiO_2 sample and TiO_2 doped with 1 wt.% of La, together with the corresponding unit cell parameters of anatase (the values in parenthesis represent estimated standard deviations), are presented in Fig. 1. These results show that value of the parameter a in both samples varies around its reference value ($a_0 = 3.78479(3)$ Å). However, the value of the c parameter is smaller than the reference one ($c_0 = 9.51237(12)$ Å), especially in La-doped sample. Decrease in c parameter value with La doping could be a consequence of the lattice contraction induced by doping. The presence of low-intensity diffraction peak at $2\theta \approx 30.8°$ that can be ascribed to the brookite phase of TiO_2 is observed in all XRD patterns (JCPDS card 29-1360).

Structure refinements were performed by the Rietveld method. Low values of agreement factors between the model, both for structure and microstructure, and XRD data indicate high accuracy of obtained results. The obtained average crystallite size and average strain in anatase and brookite phase, as well as quantitative phase analysis results (brookite content), were summarized in Table. These results showed that doping with 1 wt.% of La induced crystallite size decrease, whereas strain value and brookite content increased. The large values of the average strain in brookite crystallites indicate that this phase is highly disordered both in pure and La-doped samples.
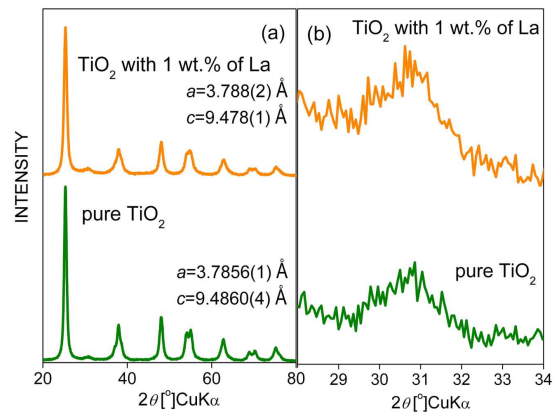

Fig. 1. (a) XRD diffractograms of pure and La-doped TiO_2 samples XRD diffractograms. (b) Enlarged diffraction peak ascribed to brookite phase.

TABLE

The results of the Rietveld analyses (average crystallite size and average strain in anatase and brookite phase) and content of brookite phase for pure TiO_2 and TiO_2 doped with 1 wt.% of La.

Samples	Anatase crystallite size [nm]	Average strain in anatase	Brookite content [%]	Brookite crystallite size [nm]	Average strain in brookite
Pure TiO_2	12	4.2×10^{-3}	16	35	19.6×10^{-3}
La-doped TiO_2	10	5.7×10^{-3}	24	26	22.0×10^{-3}

The Raman spectra of pure and La-doped TiO_2 samples produced by sol-gel method were measured at room temperature. Some of these spectra are shown in Fig. 2a. In the spectra of all TiO_2 samples the dominant Raman modes can be assigned to the Raman active modes of the anatase crystal [7]: ≈ 143 cm^{-1} ($E_{g(1)}$), 197 cm^{-1} ($E_{g(2)}$), 399 cm^{-1} ($B_{1g(1)}$), 540 cm^{-1} (combination of A_{1g} and $B_{1g(2)}$ that cannot be resolved at room temperature) and 639 cm^{-1} ($E_{g(3)}$). The position of $E_{g(1)}$ Raman mode for different TiO_2 samples ranges between 143 and 144 cm^{-1}, while its linewidth varies from 12.1 to 13.7 cm^{-1}, as can be seen in Fig. 3b.

Several factors such as phonon confinement [8–12], strain [8, 13], non-homogeneity of the particle size distribution [8, 9, 13], defects and nonstoichiometry [8, 14], as well as anharmonic effects [9, 15] can contribute to the changes in the peak position, linewidth and shape of the $E_{g(1)}$ Raman mode in anatase TiO_2 nanopowders. However, the separation between these various contributions is not straightforward [16]. Dominance of one or more of these factors, observable in the Raman spectra, is determined by the structural characteristics of a TiO_2 nanopowder: grain size and grain size distribution, existence of mixed phases (anatase in combination with considerable amount of rutile or brookite phase), value and
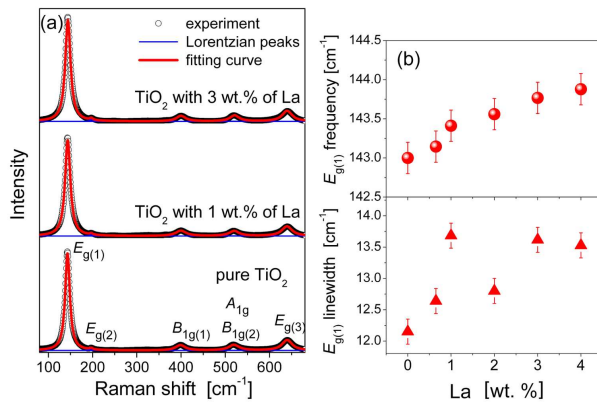
Fig. 2. (a) Raman spectra of pure and La-doped TiO$_2$ samples. (b) Frequency and linewidth of $E_{g(1)}$ Raman mode for TiO$_2$ with 0 to 4 wt.% of La. The error bars correspond to experimental error.
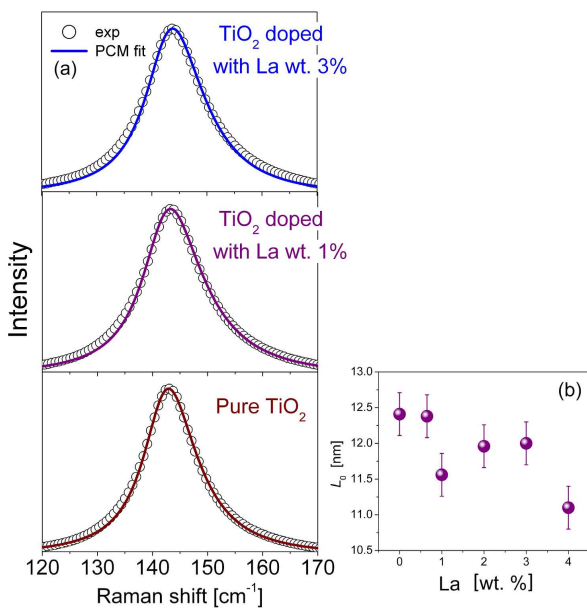

Fig. 3. (a) PCM fits of anatase $E_{g(1)}$ Raman mode for pure and La-doped samples. (b) Average particle dimensions for TiO$_2$ with 0 to 4 wt.% of La, obtained from PCM. The error bars correspond to the estimated statistical errors.

type of the strain (compressed or tensile), discrepancy from stoichiometry as well as type of defects, etc. [8]. The main factors that influence the behavior of $E_{g(1)}$ mode in our samples synthesized by sol-gel method should be the grain size and the grain size distribution, as well as the disorder induced by existence of considerable amount of brookite phase in combination with anatase and by introducing of La^{3+} ions into the TiO$_2$ lattice.

The intensities of $E_{g(1)}$ mode for different samples calculated by phonon confinement model (PCM), described in detail in our previous papers [9, 17], coincide well with

the experimental spectra, as can be seen from Fig. 3a. Average sizes of anatase nanoparticles for different TiO$_2$ samples obtained from PCM (Fig. 3b) vary from 11 to 12.4 nm and coincide well with the values obtained by XRD analyses shown in Table.

The results of the investigation of brookite phase presence by Raman spectroscopy are shown in Fig. 4. The additional Raman modes at about 243, 294, 323 and 362 cm^{-1} (shown in Fig. 4a), can be ascribed to the brookite phase of titania [17–19]. Low intensities and large widths of these modes indicate great disorder and partial amorphization of brookite in all the samples. To estimate the amount of brookite phase, the sum of the integrated intensities of Lorentzian peaks originating from the brookite modes was compared to the intensity of Lorentzian peak related to the B_{1g} mode of anatase phase. The intensity ratio of brookite modes to anatase one ($I_{B(\Sigma)}/I_{A(B1g)}$) is shown in Fig. 4a. Although these results are mainly qualitative, they confirm the results obtained by XRD analyses. It can be seen from Fig. 4b that brookite content for sample doped with 1 wt.% of La estimated from the Raman spectra are higher than the content in the pure TiO$_2$ sample. The amount of brookite phase for the samples with the other values of La wt.% is similar to the value in pure TiO$_2$.
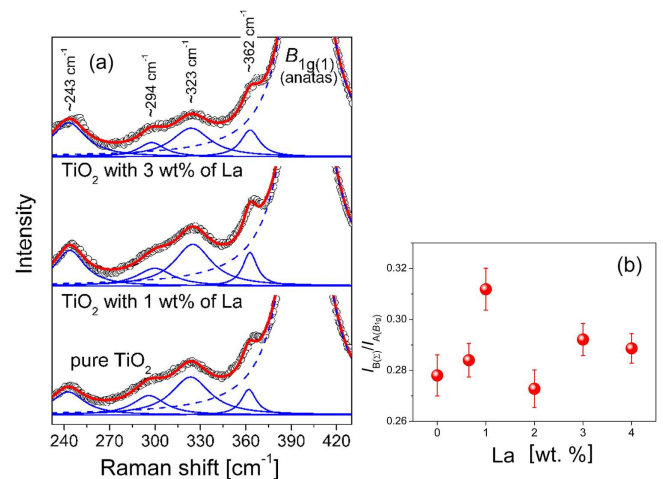

Fig. 4. (a) Lorentzian fits of brookite modes in the experimental Raman spectra. (b) The ratio of the total brookite modes intensity and the anatase B_{1g} Raman mode intensity for TiO$_2$ with 0 to 4 wt.% of La. The error bars correspond to the errors obtained by fit analysis.

It is well known that the phase transition from anatase to rutile occurs at $\approx 600°$C. In order to investigate the influence of La doping on phase stability of nanostructured TiO$_2$, pure TiO$_2$ and TiO$_2$ doped with 3 wt.% of La were treated at high temperatures up to 800°C. The Raman spectra of these samples, before and after thermal treatment, are shown in Fig. 5. It could be observed that the heating of pure TiO$_2$ to 800°C causes redshift and narrowing of anatase E_g Raman mode which im-
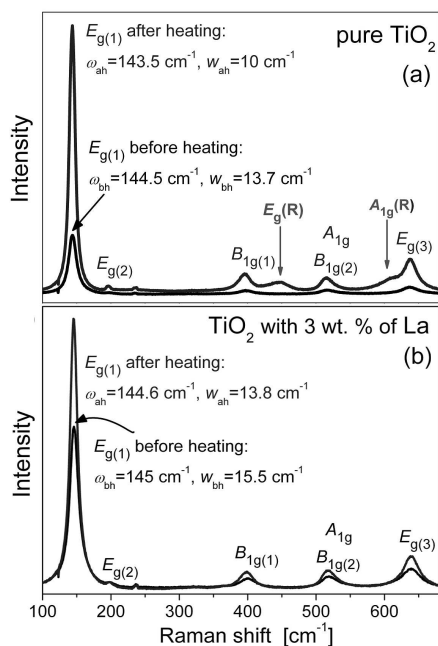
Fig. 5. Raman spectra of pure TiO₂ and TiO₂ doped with 3 wt.% of La at room temperature before and after heating to 800°C. ω is the mode frequency and w is the linewidth of $E_{g(1)}$ Raman mode before (bh) and after (ah) heating. R denotes rutile modes.

plies anatase crystallite growth. Also, the appearance of the new Raman modes assigned to rutile phase was registered. After the same heating treatment of the La-doped sample neither such drastic changes of E_g Raman mode nor the appearance of peaks in the spectrum, belonging to rutile phase, were registered. This allowed us to conclude that La doping stabilized TiO₂ nanostructure at high temperatures and shifted the temperature of anatase–rutile phase transition to values higher than 800°C.

4. Conclusion

A detailed Raman study of sol-gel synthesized anatase TiO₂ nanopowders doped with lanthanum ions (La³⁺) in the range from 0 to 4 wt.% was presented in this paper. It was demonstrated that the frequency shift and broadening of the most intensive anatase $E_{g(1)}$ Raman mode are the consequences of both confinement effect due to the nanosize dimensions of anatase crystallites and the disorder induced by the presence of brookite phase and La dopant in the samples. This enables not only basic phase identification but also the estimation of the nanoparticles size and brookite contents in TiO₂ nanopowders with different La content.

This study allows us to investigate the structural variations of nanosized TiO₂ arisen from the change in doping conditions and it confirms that doping of TiO₂ by La³⁺ ions significantly improves phase and nanostructure stability of TiO₂ powders at high temperatures.

References

[1] S. Sakka, *J. Sol-Gel Sci. Technol.* **37**, 135 (2006).

[2] J.N. Hart, D. Menzies, Y.-B. Cheng, G.P. Simon, L. Spiccia, *J. Sol-Gel Sci. Technol.* **40**, 45 (2006).

[3] D. Kim, A. Rothschild, D.-J. Yang, H.L. Tuller, *Sensor Actuat. B-Chem.* **130**, 9 (2008).

[4] C.G. Granqvist, A. Azens, J. Isidorsson, M. Kharrazi, L. Kullman, T. Lindström, G.A. Niklasson, C.-G. Ribbing, D. Rönnow, M. Strømme Mattsson, M. Veszelei, *J. Non-Cryst. Solids* **218**, 273 (1997).

[5] J. Rodriguez-Carvajal, 1998, FullProf computer program; ftp://charybde.saclay.cea.fr/pub/divers/fullprof.98/windows/winfp98.zip .

[6] A. Kremenovic, J. Blanusa, B. Antic, Ph. Colomban, V. Kahlenberg, C. Jovalekic, J. Dukic, *Nanotechnology* **18**, 145616 (2007).

[7] T. Ohsaka, F. Izumi, Y. Fujiki, *J. Raman Spectrosc.* **7**, 321 (1978).

[8] M.J. Šćepanović, M.U. Grujić-Brojčin, Z.D. Dohčević-Mitrović, Z.V. Popović, *Mater. Sci. Forum* **518**, 101 (2006).

[9] M.J. Šćepanović, M. Grujić-Brojčin, Z. Dohčević-Mitrović, Z.V. Popović, *Appl. Phys. A* **86**, 365 (2007).

[10] D. Bersani, P.P. Lottici, *Appl. Phys. Lett.* **72**, 73 (1998).

[11] H. Richter, Z.P. Wang, L. Ley, *Solid State Commun.* **39**, 625 (1981).

[12] I.H. Campbell, P.M. Fauchet, *Solid State Commun.* **58**, 739 (1984).

[13] J.E. Spanier, R.D. Robinson, F. Zhang, S.W. Chan, I.P. Herman, *Phys. Rev. B* **64**, 245407 (2001).

[14] J.C. Parker, R.W. Siegel, *Appl. Phys. Lett.* **57**, 943 (1990).

[15] K.R. Zhu, M.S. Zhang, Q. Chen, Z. Yin, *Phys. Lett. A* **340**, 220 (2005).

[16] G. Gouadec, P. Colomban, *Prog. Cryst. Growth Charact. Mater.* **53**, 56 (2007).

[17] A. Golubović, M. Šćepanović, A. Kremenović, S. Aškrabić, V. Berec, Z. Dohčević-Mitrović, Z.V. Popović, *J. Sol-Gel Sci. Technol.* **49**, 311 (2009).

[18] Y. Djaoued, R. Brüning, D. Bersani, P.P. Lottici, S. Badilescu, *Mater. Lett.* **58**, 2618 (2004).

[19] S. Yin, K. Ihara, B. Liu, Y. Wang, R. Li, T. Sato, *Phys. Scr. T* **129**, 268 (2007).